

## On-chip recalcification of citrated whole blood using a microfluidic herringbone mixer

Marcus Lehmann, Alison M. Wallbank, Kimberly A. Dennis,  
Adam R. Wufsus, Kara M. Davis, Kuldeepsinh Rana, and Keith B. Neeves<sup>a)</sup>  
*Chemical and Biological Engineering Department, Colorado School of Mines, Golden,  
Colorado 80401, USA*

(Received 11 September 2015; accepted 2 November 2015; published online 18 November 2015)

*In vitro* assays of platelet function and coagulation are typically performed in the presence of an anticoagulant. The divalent cation chelator sodium citrate is among the most common because its effect on coagulation is reversible upon reintroduction of divalent cations. Adding divalent cations into citrated blood by batch mixing leads to platelet activation and initiation of coagulation after several minutes, thus limiting the time blood can be used before spontaneously clotting. In this work, we describe a herringbone microfluidic mixer to continuously introduce divalent cations into citrated blood. The mixing ratio, defined as the ratio of the volumetric flow rates of citrated blood and recalcification buffer, can be adjusted by changing the relative inlet pressures of these two solutions. This feature is useful in whole blood assays in order to account for differences in hematocrit, and thus viscosity. The recalcification process in the herringbone mixer does not activate platelets. The advantage of this continuous mixing approach is demonstrated in microfluidic vascular injury model in which platelets and fibrin accumulate on a collagen-tissue factor surface under flow. Continuous recalcification with the herringbone mixer allowed for flow assay times of up to 30 min, more than three times longer than the time achieved by batch recalcification. This continuous mixer allows for measurements of thrombus formation, remodeling, and fibrinolysis *in vitro* over time scales that are relevant to these physiological processes.  
© 2015 AIP Publishing LLC. [<http://dx.doi.org/10.1063/1.4935863>]

### I. INTRODUCTION

The formation of a blood clot is intimately tied to the local hemodynamics at the site of a vascular injury.<sup>1</sup> Platelet adhesion and aggregation, and von Willebrand factor function are shear stress dependent events.<sup>2,3</sup> Platelet agonists, coagulation factors, and fibrin polymerization are subject to mass transfer limitations that regulate clot growth and structure.<sup>4–6</sup> To study these biophysical phenomena, parallel plate, microfluidic, and microcapillary flow chambers—collectively referred to as flow assays—are often used to study the dynamics of clot formation typically over a time scale of 1–10 min.<sup>7–15</sup> In these assays, whole blood is perfused over prothrombotic substrates that mimic components of the vessel wall including adhesive proteins such as collagen and initiators of coagulation, such as tissue factor (TF). Alternatively, microfluidic devices have been reported that miniaturize common clinical assays such as prothrombin time (PT) and activated partial thromboplastin time (aPTT) using plasma<sup>16</sup> or whole blood.<sup>17–19</sup> However, these devices do not impose the same mass transfer limitations that regulate coagulation in blood clots formed on vessel walls under flow.<sup>4,20</sup>

A necessary compromise for removing blood from the body for all these assays is that blood is typically collected into anticoagulants which irrevocably alters platelet function and

---

<sup>a)</sup> Author to whom correspondence should be addressed. Electronic mail: [kneeves@mines.edu](mailto:kneeves@mines.edu). Tel. (Office): (303) 273-3191. FAX: (303) 273-3730.

coagulation.<sup>21,22</sup> The most common anticoagulant is sodium citrate because it can be partially reversed by mixing divalent cations, primarily calcium and magnesium, back into the blood. For microfluidic chambers, it is ideal to conduct this mixing on-chip in order to reduce blood volumes. However, in addition to the well-documented challenges of mixing in low Reynolds number flows,<sup>23–25</sup> mixing with whole blood is further hindered by the low diffusivity of suspended blood cells. In this report, we describe a method for continuous on-chip recalcification of sodium citrate anticoagulated whole blood, hereafter referred to as citrated blood, for microfluidic flow assays.

The method of mixing divalent cations into citrated whole blood ultimately limits flow assay duration. The simplest approach is batch mixing, which introduces a single bolus of divalent cations into the citrated blood prior to the assay.<sup>9</sup> As soon as the divalent cations are added to the blood, platelets can activate and coagulation will initiate.<sup>21</sup> Moreover, in batch mixing, the time from the addition of divalent cations to the time that blood contacts the prothrombotic substrate in the flow assay varies over the duration of the assay. As such, platelets at the end of the assay may be partially activated and more likely to aggregate than at the beginning of the assay. One approach to extend flow assay duration is semi-batch mixing where aliquots of recalcified blood are introduced into a flow chamber so that the blood is recalcified for no longer than a few minutes.<sup>14</sup> Another alternative is continuous mixing of divalent cations and citrated whole blood upstream of the prothrombotic substrate. For example, a tubing Y-junction placed upstream of the inlet of a flow chamber can be used to combine citrated whole blood and a solution of divalent cations at a user-defined volume ratio.<sup>11</sup> An upstream mixing chamber with an incorporated stir bar can be used to mix agonist solutions, but could potentially activate platelets even without agonists<sup>26</sup> and also requires large volumetric flow rates. These mixing strategies are suitable for larger flow chambers that use milliliters of blood where the dead volume in connectors, mixers, and tubing are not significant. However, on-chip mixing is preferable in microfluidic chambers that use microliters of blood where such dead volumes are prohibitive. A summary of the various mixing strategies and their applications is given in Table I.

Mixing in microfluidic devices poses several well-documented challenges<sup>24,25,27</sup> due to low Reynolds number flows and high Péclet numbers. For a solution or suspension to be well mixed, there must be no concentration gradients. Concentration gradients are eliminated by diffusion, which is slow relative to convection, scaling with the square root of time. Thus, to increase mixing speed, the diffusion length needs to be shortened. However, it is difficult to decrease the diffusion length in low Reynolds number flows in long channels with straight walls because flow is smooth and laminar. One on-chip mixing strategy is a sheath flow where two recalcification streams are brought in adjacent to either side of a stream of citrated blood.<sup>28</sup> Another strategy is chaotic advective mixing, where the diffusion length becomes exponentially smaller by stretching and folding a fluid. Stroock *et al.* elegantly demonstrated this type of mixing by integrating staggered herringbone reliefs into one wall of a microfluidic channel.<sup>27</sup> Mixing blood is further constrained by the fact that channel dimensions must be large enough to avoid altering the hematocrit (Fahreus effect), and the shear stresses must be small enough to avoid shear induced platelet activation.<sup>29</sup>

In this report, we describe a herringbone mixer to continuously mix divalent cations and citrated whole blood for measuring platelet function and coagulation in flow assays. We show that we can mix citrated blood and a recalcifying buffer at a user-defined mixing ratio without activating platelets. The utility of the mixer is demonstrated by prolonging the duration of flow assays from 7 min by batch mixing to 30 min by continuous mixing.

## II. MATERIALS AND METHODS

### A. Materials

Human type I fibrillar collagen was from Chrono-Log Corp (Havertown, PA). Calcium chloride, sodium chloride, magnesium chloride, adenosine diphosphate (ADP), paraformaldehyde, and 3,3'-dihexyloxycarbocyanine iodide (DiOC6) were purchased from Sigma-Aldrich (St. Louis, MO). Tridecafluoro-1,1,2,2-tetrahydrooctyl) trichlorosilane was from Gelest (SIT8174.0, Morrisville, PA).

TABLE I. Summary of mixing methods for introducing divalent cations into citrated whole blood.

Mixing method	Advantages	Disadvantages
Herringbone Mixer: On-chip herringbone features induce chaotic advective mixing of recalcification solution and whole blood.	<ul style="list-style-type: none"> <li>• Continuous mixing</li> <li>• Flexible mixing ratios</li> <li>• Can be connected in series to independent flow chambers</li> <li>• Allows for long assay time (30 min)</li> </ul>	<ul style="list-style-type: none"> <li>• Easy to trap air bubbles</li> <li>• Requires additional inlet and outlet connections and tubing</li> </ul>
Batch: A single bolus of recalcification solution is added to blood prior to perfusion. <sup>20</sup>	<ul style="list-style-type: none"> <li>• Simplicity, no additional channels or tubing required</li> </ul>	<ul style="list-style-type: none"> <li>• Limited to short assays (~5 min)</li> <li>• Variable time from recalcification to contact with injury site</li> </ul>
Semi-batch: Reservoir of recalcified blood replaced by fresh aliquots every few minutes. <sup>14</sup>	<ul style="list-style-type: none"> <li>• Simplicity, no additional channels or tubing required</li> <li>• Prolonged assay time relative to batch.</li> </ul>	<ul style="list-style-type: none"> <li>• Frequent fluid changes increase chance of user error.</li> <li>• Variable time from recalcification to contact with injury site</li> </ul>
Sheath flow: Two streams of recalcification buffer adjacent to blood. <sup>28</sup>	<ul style="list-style-type: none"> <li>• Continuous mixing</li> <li>• Useful for studying calcium/drug gradients and incubation time.</li> </ul>	<ul style="list-style-type: none"> <li>• Passive diffusive mixing requires long channels</li> <li>• Degree of mixing and hematocrit varies along channel</li> </ul>
Y-junction: Y-connector used to bring recalcification solutions and whole blood together off-chip. <sup>11</sup>	<ul style="list-style-type: none"> <li>• Simple off-the-shelf tubing attachment</li> </ul>	<ul style="list-style-type: none"> <li>• Large dead volume</li> <li>• Requires two independent pumps</li> </ul>
Stir bar chamber: On-chip reservoir with a stir bar. <sup>26</sup>	<ul style="list-style-type: none"> <li>• Can mix a several different solutions</li> <li>• Continuous mixing</li> </ul>	<ul style="list-style-type: none"> <li>• Large dead volume only suitable for larger flow chambers</li> <li>• Requires two independent pumps</li> </ul>

One micrometer polystyrene beads (505/515) were from Life Technologies (Cat #F8765, Carlsbad, CA). Tubing (Tygon S-54-HL PVC Medical Tubing, 0.010" ID) was from Cole Parmer (Vernon Hills, IL). Polydimethylsiloxane (PDMS, Dow Corning Sylgard 184) was from Krayden (Westminster, CO). Sterile 0.1  $\mu\text{m}$  filtered phosphate buffer saline (PBS) was from Hyclone (Logan, UT). The photoresist KMPR 1050 was from MicroChem (Newton, MA). Fluorescein isothiocyanate (FITC) anti-human PAC-1 (CD41/CD61) and Allophycocyanin (APC) anti-human CD62P were from BioLegend (Cat # 362803, #304910 San Diego, CA). Alexa 555 protein labeling kit was from Life Technologies (Carlsbad, CA) and was used according to the manufacturer's instruction to label fibrinogen (1.4 mg/ml). TF was purchased from Innovin (Siemens, Erlangen, Germany). HEPES buffered saline (HBS; 20 mM HEPES, 150 mM NaCl, pH 7.4), recalcification buffer (75 mM  $\text{CaCl}_2$ , 37.5 mM  $\text{MgCl}_2$  in HBS), and bovine serum albumin buffer (BSA buffer; 2 mg/ml BSA in HBS) were made in-house.

## B. Device design and fabrication

The mixing device consisted of a microfluidic channel (height = 50  $\mu\text{m}$  and width = 1800  $\mu\text{m}$ ) with bas-relief herringbone structures (depth = 50  $\mu\text{m}$ ) in the top of the channel capable of inducing transverse flows within the microfluidic channel (Fig. 1(a)). The herringbone grooves were 50  $\mu\text{m}$  wide and 50  $\mu\text{m}$  tall and alternating 250  $\mu\text{m}$  and 150  $\mu\text{m}$  long, pitched at 45° from the direction of flow and 90° from each other. The herringbone pattern was 600  $\mu\text{m}$  in width and three repeats stacked together extended the width of the channel. The groove structures were spaced 50  $\mu\text{m}$  apart, and sets of five were mirrored and offset by 30  $\mu\text{m}$ . A total of twelve structures spanned the length of the 3 cm long channel. The device has two inlets: inlet 1 for the blood and inlet 2 for the recalcification buffer. Inlet 1 splits into two parallel microfluidic channels that are 500  $\mu\text{m}$  wide, 50  $\mu\text{m}$  tall, and each 16.5 mm long that join the channel from inlet 2 at node B (Fig. 1(b)). Inlet 2 connects to a

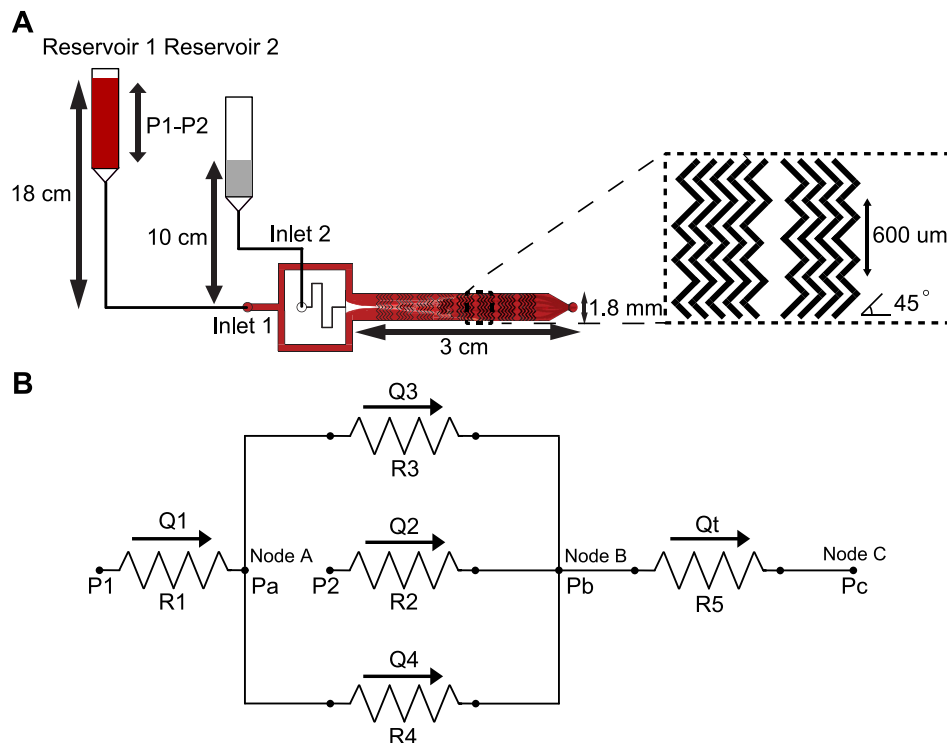


FIG. 1. Schematic of mixing device set up for recalcification. (a) Inlet 1 is used for blood and inlet 2 is used for the recalcification buffer. The difference in heights of the inlet reservoirs dictates difference in head pressure ( $P_1 - P_2$ ) that controls the flow rate ratio. With whole blood, reservoir 1 is set to 18 cm and reservoir 2 is set to 10 cm to give a 9:1 flow rate ratio. (b) Resistor network analogy for hydraulic circuit analysis of the mixing device.

microfluidic channel that is  $50\ \mu\text{m}$  wide,  $50\ \mu\text{m}$  tall, and  $13.4\ \text{mm}$  long. These channels define inlet resistances  $R_1$ ,  $R_2$ ,  $R_3$ , and  $R_4$ , as shown in Fig. 1(b). A vacuum chamber surrounds the channels to aid in the removal of bubbles during priming of the chamber with buffer. Hydraulic circuit analysis<sup>30</sup> was used to determine the difference in head pressures needed for a given dilution ratio (Fig. 1(b)). The device was sealed to a glass slide via plasma-assisted bonding. The device master was fabricated using the photoresist KMPR 1050. A first layer of the photoresist was spun on a silicon wafer (3000 RPM), soft-baked at  $100^\circ\text{C}$  for 15 min, and subsequently exposed to UV light ( $1000\ \text{mJ}/\text{cm}^2$ ) through a Mylar mask that defined the channel pattern. This wafer was then hard-baked at  $100^\circ\text{C}$  for 3 min before a second layer of photoresist was spun at 3000 RPM. The second layer was exposed ( $1000\ \text{mJ}/\text{cm}^2$ ) to a pattern consisting of the herringbone groove pattern aligned to the bottom layer. The wafer was hard baked at  $100^\circ\text{C}$  for 3 min and then developed in 2.38% tetramethylammonium hydroxide (AZ 300 MIF). The height of each layer was  $48\text{--}52\ \mu\text{m}$ . The master was treated with (tridecafluoro-1,1,2,2-tetrahydrooctyl) trichlorosilane under vacuum for 4 h. Polydimethylsiloxane was poured on the wafer at a 10:1 ratio of base to catalyst and the wafer was cured in a convection oven for 4 h at  $60^\circ\text{C}$ . The mold was peeled and inlet and outlet holes ( $0.75\ \text{mm}$ ) and a vacuum hole ( $1.5\ \text{mm}$ ) were defined with a biopsy punch (World Precision Instruments, Sarasota, FL, Cat #504529; Ted Pella, Redding, CA, Cat #15110-15).

### C. Device operation

Two operating modes were used to characterize the performance of the mixer. In pull mode (Fig. 2(a)), two fluid reservoirs were connected to inlets 1 and 2 of the mixer with tubing (20 cm, Tygon S-54-HL PVC Medical Tubing, 0.01" ID, Cat #EW-06419-00). The outlet of the mixer was connected to the flow device by 75 cm of tubing. The flow device consists of microfluidic channels running parallel to a micropatterned strip of a prothrombotic substrate (described in Sec. IIH). The flow device was connected to a 1 ml Hamilton Gastight syringe (#81320) on a syringe pump by 20 cm of tubing. The syringe pump then controls the total fluid flow rate by pulling the solutions through the mixer and flow device. The mixing ratio was controlled by the relative heights of the reservoirs. In push mode (Fig. 2(b)), two syringes with different solutions were placed on a single syringe pump and connected to the mixer with 20 cm of tubing. The mixer was connected to the flow device and the outlet of the flow device was connected to a waste or sample collection tube. In this mode, the syringe pump controlled the flow rates and the mixing ratio was controlled by the ratio of cross sectional areas of the syringes used for the perfusion. For a 10:1 mixing ratio, we used 1 ml (ID = 4.61 mm) and  $100\ \mu\text{l}$  (# 81020, ID = 1.46 mm) Hamilton Gastight syringes in conjunction.

### D. Blood collection and labeling

Blood was collected from healthy donors by venipuncture into 4.5 ml vacutainer tubes containing 3.2% sodium citrate. Phlebotomy was conducted in accordance with the Declaration of Helsinki and the Institutional Review Board of the University of Colorado, Boulder. Donors

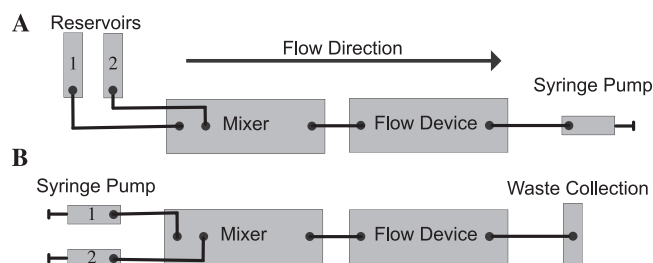


FIG. 2. Schematic of the two modes of device operation. (a) Pull-mode. Reservoirs are connected to the inlets of the mixer. The mixer is connected to the flow device, and the flow device is connected to a syringe on a syringe pump. The syringe pulls the fluids through at a set combined flow rate. (b) Push-mode. Syringes on a syringe pump are connected to the mixer inlets. The mixer is connected to a flow device, and the flow device is connected to waste collection.

had neither consumed alcohol within 48 h prior to the draw nor had they taken any prescription or over-the-counter drugs within the previous 10 days, excluding oral contraception. The first tube of blood collected was discarded to eliminate any activated platelets due to venipuncture. Hematocrit was measured with a CritSpin (Beckman Coulter, Brea, CA) following the manufacturer's instructions. For each flow assay, 1 ml whole blood was aliquoted into 1.5 ml centrifuge tubes containing 1  $\mu$ l of the DiOC6 (final concentration 1  $\mu$ M) and 40  $\mu$ l of the labeled fibrinogen (final concentration 56  $\mu$ g/ml). The aliquots were placed in a 37 °C water bath for 15 min to resensitize platelets.<sup>11</sup>

### E. Measurement of platelet activation by flow cytometry

Platelet activation measurements were performed using the mixer in push mode (Fig. 2(b)). One milliliter and 100  $\mu$ l Hamilton Gastight syringes were filled with citrated whole blood and recalcification solution, respectively, and connected to the mixer inlets 1 and 2. The mixture was perfused at a blood flow rate of 8.9  $\mu$ l/min and recalcification buffer flow rate of 0.89  $\mu$ l/min. The outlet was collected into 300  $\mu$ l of PBS every 10 min. The samples were centrifuged at 200 g for 5 min. The top fraction of platelet rich plasma (PRP) was collected and placed into a 1.5 ml microcentrifuge tube. The sample was then fixed with 0.5% paraformaldehyde. Antihuman PAC-1 antibody (5  $\mu$ l, FITC) or CD62P antibody (5  $\mu$ l, APC) was added and incubated in the dark overnight at 4 °C. Samples were diluted to a final volume of 1 ml and analyzed via flow cytometry (Guava EasyCyte, Merck, Darmstadt, Germany). For the positive and negative controls, 15  $\mu$ l of whole blood was diluted into 300  $\mu$ l of PBS and centrifuged at 200 g for 5 min. The resultant PRP was pipetted into a 1.5 ml microcentrifuge tube. As a positive control for platelet activation, 10  $\mu$ l human  $\alpha$ -thrombin (final concentration 0.3  $\mu$ M) or 30  $\mu$ l ADP (final concentration 50  $\mu$ M) was added to the PRP, followed by a 2 (PAC-1) or 60 (CD62P) min incubation without agitation. The sample was fixed with 0.5% paraformaldehyde. For the negative control, no thrombin or ADP was added. PAC-1 or CD62P was used to label activated platelets as described above. The controls were then diluted to a final volume of 1 ml prior to testing. The platelet population was gated based on the forward-side scatter to discriminate platelets from leukocytes and erythrocytes. Platelet activation was reported as the fraction of PAC-1 and CD62P positive platelets.<sup>31</sup>

### F. Quantification of mixing

A suspension of 1  $\mu$ m polystyrene beads (0.2 wt. %, inlet 1) and PBS (inlet 2) were perfused through the mixer device in the presence and in the absence of herringbone grooves in pull mode (Fig. 2(a)). These two solutions were perfused at total volumetric flow rates of 1.2, 8.9, and 30  $\mu$ l/min with a 9:1 (bead suspension:PBS) ratio. Images of the beads (Olympus IX-81, 2X NA=0.06, ex/em 490/510) were taken along the mixer every 1.5 mm. Mixing was quantified by measuring the standard deviation of the fluorescent intensity across the image of the channel using ImageJ software<sup>32</sup> and normalizing by the standard deviation at the beginning of the mixer. Mixing with whole blood and recalcification buffer was visualized with brightfield images taken at nodes B and C (Fig. 1(b)) as well as at the location of the collagen-TF strip in the flow device channel.

### G. Control of mixing ratio

To quantify the mixing ratio, the mixer was run in pull mode (Fig. 2(a)). A reservoir of 30% glycerol mixed with food dye was used to mimic the bulk viscosity of whole blood (3–4 cP at room temperature) and connected to inlet 1. Glycerol was used instead of blood in order to avoid trace amounts of excess calcium or sodium citrate from the blood draw interfering with the calcium ion measurements. Recalcification buffer was connected to the inlet 2. A 1 ml syringe was connected to the outlet of a mixer and was used to pull and collect the solutions at a total flow rate of 8.9  $\mu$ l/min. The recalcification buffer reservoir was maintained at a height of 8 cm and the height of the glycerol solution was adjusted to vary the width of the recalcification

stream, which was measured by bright field microscopy just prior to the first relief structure. 900  $\mu\text{l}$  of the effluent was collected at the outlet and added to 19.1 ml of deionized water (18.2 M $\Omega$ ). The calcium concentration of the diluted effluent was measured using a Vernier Calcium Probe (cat# CA-BTA, Beaverton, OR). This concentration was used to calculate the dilution ratio of the calcium ions from the solution introduced through inlet 2.

#### H. Whole blood flow assay

Type I fibrillar collagen (500  $\mu\text{g}/\text{ml}$ ) and TF (3.68 nM) were patterned on a clean glass slide by filling a microfluidic channel ( $w = 150 \mu\text{m}$ ,  $h = 50 \mu\text{m}$ ) with the solution and allowing it to incubate on the surface for 45 min.<sup>33,34</sup> The patterning device was peeled off along the axis of the channel and the surface gently rinsed with deionized water (18.2 M $\Omega$  cm). The pattern was stored at 4 °C and used within 24 h. The flow assay device consisted of three parallel microfluidic channels ( $w = 500 \mu\text{m}$ ,  $h = 50 \mu\text{m}$ ) with separate inlets and outlets and vacuum bonded to the slide containing the collagen-TF strip.<sup>9</sup> The mixer was oxygen plasma bonded to a clean glass slide at least 24 h prior to use to allow for complete bonding.<sup>35</sup> A 5 ml reservoir of 2% BSA buffer was connected to inlet 1 of the mixer with 20 cm of tubing. A 3 ml reservoir of recalcification buffer was connected to inlet 2 of the mixing device with 20 cm of tubing. The BSA reservoir and recalcification buffer reservoir were placed 18 cm and 10 cm above the mixing device, respectively. The outlet of the mixer was connected to the flow assay device with 75 cm of tubing (0.256 mm ID). The outlet of the flow assay device was connected to a 1 ml syringe, and the solutions were withdrawn at 1  $\mu\text{l}/\text{min}$  for at 45 min prior in order to block non-specific protein adhesion. If air bubbles formed during filling, a vacuum pump could be connected to the mixer via tubing (0.512 mm ID). The vacuum accelerated removal of bubbles. The BSA solution was replaced with the labeled citrated whole blood and a total flow rate of 8.9  $\mu\text{l}/\text{min}$  was withdrawn, corresponding to an initial wall shear rate of 750  $\text{s}^{-1}$  in the flow assay channel. Platelet and fibrin accumulation were captured by relief contrast microscopy and epifluorescence microscopy (Olympus IX81, 20X NA=0.45, ex/em 475/505, 545/580) at 10 frames/min. The blood in the reservoir was mixed via gentle aspiration with a transfer pipette every 10 min to prevent RBC settling. Blood was used within 90 min of phlebotomy. Flow assays using batch recalcification were also performed; a 900  $\mu\text{l}$  aliquot of whole blood was mixed with 100  $\mu\text{l}$  of the recalcification buffer immediately prior to perfusion through the flow assay device.

#### I. Measurements of accumulation of fibrinogen and platelets in the mixer

The mixer was set up in identical fashion to the *Whole Blood Flow Assay* (Sec. II H) except the outlet was connected directly to syringe pump instead of to a flow assay device. Citrated whole blood and recalcification buffer were withdrawn at 8.9  $\mu\text{l}/\text{min}$  at a 1:10 dilution ratio. Platelet and fibrin accumulation were captured by relief contrast microscopy and epifluorescence microscopy, respectively, at 1 frame/min at six locations in the mixer for 30 min. After 30 min. the whole blood was replaced with 2% paraformaldehyde in HBS and the mixer was inspected for platelet accumulation.

#### J. Data analysis

Flow cytometry data was gated with FlowJo software (v.10, FlowJo LLC, Ashland, OR). Statistical significance at a significance level of  $\alpha = 0.05$  for the platelet activation was tested with one-way analysis of variance (ANOVA) followed by Tukey's post-test for flow cytometry data. Image analysis for the bead mixing was performed with ImageJ software by selecting a line perpendicular to the direction of flow and spanning the width of the channel after every groove set. The standard deviation of the fluorescent intensity of the line is taken to be an indicator of mixing. The standard deviation was normalized by the initial standard deviation of the unmixed solutions to define a mixing index (MI)

$$MI = \frac{\sqrt{\sum_{i=1}^N (x_i - \mu)^2}}{\sqrt{\sum_{i=1}^N (x_{i,0} - \mu_0)^2}}, \quad (1)$$

where  $x_i$  is the fluorescent intensity of the individual pixel along the line;  $\mu$  is the mean fluorescent intensity of the line;  $N$  is the total number of pixels; and  $x_{i,0}$ , and  $\mu_0$  designating the measurement of the premixed condition. Image analysis of the whole blood flow assays was performed with ImageJ software by measuring the integrated fluorescent signal of the field-of-view for each frame and was expressed in integrated fluorescent units (IFU). Relief contrast images from the flow assays were analyzed using a custom Sobel-based MATLAB image edge finding routine.<sup>7</sup> This routine measures the area fraction occupied by platelets on the collagen strip. The lag time for each flow assay was defined as the time to reach 5% surface coverage as measured by the relief contrast.<sup>7,9</sup> The growth rate was defined as the slope of the linear growth regime. Image analysis for the protein and platelet accumulation was performed using ImageJ software. The average fluorescence intensity of each time point was normalized by the  $t = 0$  min time point.

### III. RESULTS AND DISCUSSION

#### A. Quantification of mixing

For the purposes of recalcification of citrated whole blood, a mixer needs (i) to homogenize the suspension (blood) and the solution (divalent cations) and (ii) to provide a user-defined mixing ratio.

The homogenization criterion was measured with suspensions of model particles (1  $\mu\text{m}$  polystyrene) and whole blood (Eq. (1)). In the experiments, the suspension was introduced through inlet 1 and a buffer solution through inlet 2. Fig. 3(a) shows how distinct the two streams appear when brought together at node B and how they became dispersed by the end of the mixer. At a flow rate of 8.9  $\mu\text{l}/\text{min}$ , the bead suspension was mixed 10 mm downstream of the first herringbone feature (Fig. 3(d)). Without herringbone groves, little mixing occurred (Fig. 3(b)). Experiments with whole blood and buffer showed similar behavior (Fig. 3(c)). Similar mixing was observed at the end of the mixer at flow rates 1.2 to 30  $\mu\text{l}/\text{min}$ , which yields a range of wall shear rates in the flow chamber representative of venous to arterial blood vessels (Supplementary Fig. 2).<sup>41</sup> When the reservoirs feeding into the inlet were open to the atmosphere, which was the case for pull mode (Fig. 2(a)), the relative flow rates of the two solutions were determined by the hydraulic resistance in the tubing and channel leading up to the mixing channel and their inlet pressures. A challenge with using whole blood in pull mode (A) is that the hematocrit, and thus the viscosity, of blood varies between donors. While the average hematocrit of donors ( $n = 10$ ) in this study was 0.45, the values ranged from 0.38–0.54, corresponding to a range of relative viscosities of 1.5–2.2.<sup>36,37</sup> In order to accommodate differences in viscosities while keeping the mixing ratio constant, we changed the relative heights of the reservoirs. To monitor the mixing ratio, the width of the recalcification buffer stream,  $W_c$ , was measured at the inlet (Fig. 3(c)) and the relative height of the two reservoirs was changed to give the desired width. We defined the dilution ratio as the width of the solution introduced through inlet 2 (recalcification buffer) to the total channel width (1800  $\mu\text{m}$ ), which corresponds to the flow rate ratio

$$\text{Dilution Ratio} = \frac{W_c}{W_t} = \frac{Q_c}{Q_t}, \quad (2)$$

where  $Q_c$  is the volumetric flow rate of the recalcification buffer,  $Q_t$  is the total flow rate,  $W_c$  is the width of the recalcification buffer, and  $W_t$  is the total width of the channel.



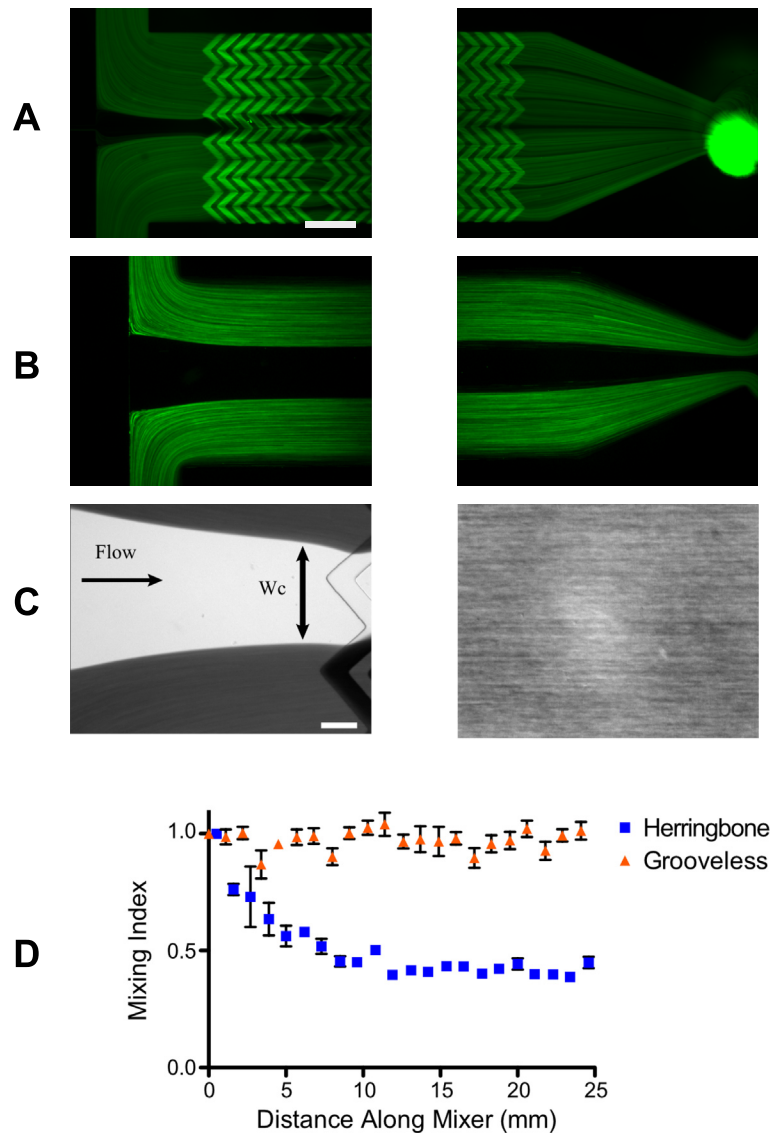


FIG. 3. Quantification of mixing. The mixing of a suspension of 0.2 wt. % fluorescent  $1\ \mu\text{m}$  beads with PBS at node B (left) and node C (right) of a device with (a) and without (b) herringbone features. Scale bar = 0.5 mm. (c) The mixing of citrated blood and recalcification buffer at node B (left) and node C (right) of a device with herringbone features. The width of the recalcification stream is  $W_c$ . Scale bar =  $100\ \mu\text{m}$ . (d) Mixing index measured along the mixing device with and without the herringbone grooves for the mixing of  $1\ \mu\text{m}$  beads with PBS ( $n = 3$ , error bars = standard deviation).

Fig. 4 shows how the dilution ratio can be adjusted by manipulating the relative height of the recalcification buffer reservoir, and thus the stream width of the recalcification ( $W_c$ ). Here, the device was run in pull mode (a) with a reservoir of 30% glycerol and food dye in HBS (used as a blood mimic) attached to inlet 1 and recalcification buffer to inlet 2. The measured calcium concentration of the samples was in good agreement with Eq. (2). Accordingly, for whole blood flow assays, the reservoirs were adjusted to give a dilution ratio of 0.1, which corresponds to a recalcification buffer stream width,  $W_c$ , of  $165\ \mu\text{m}$ . The calculation of the head pressure difference needed for a given dilution ratio for pull mode (A) is based off hydraulic circuit analysis to determine channel resistance under pressure driven flow.<sup>30</sup> The resistance of channels with a rectangular cross section was calculated by

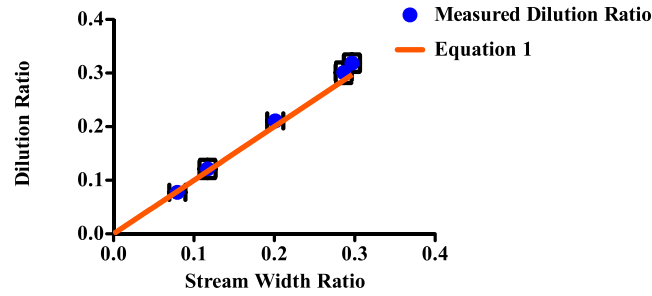


FIG. 4. Correlation between dilution ratio and stream width ratio. Experimentally measured stream width ratio ( $W_c/W_t$ ) plotted against the dilution ratio ( $Q_c/Q_t$ ) measured calcium concentration at the outlet, normalized to the inlet calcium ion concentration in Inlet 2. Without slip and both streams flowing, Eq. (2) predicts that the width ratio is the volumetric flow ratio. Error bars represent standard deviation ( $n = 3$ ).

$$R_{channel} = \frac{12\mu l}{wh^3} \left[ 1 - \frac{192h}{\pi^5 w} \sum_{n=1,3,5}^{\infty} \frac{\tanh\left(\frac{n\pi w}{2h}\right)}{n^5} \right]^{-1}. \quad (3)$$

Resistance from the tubing connection was calculated from the Hagen-Poiseuille relationship

$$R_{tubing} = \frac{128\mu l}{\pi d^4}. \quad (4)$$

Solving the hydraulic circuit (Fig. 1(b)) for the difference in pressure of the two inlets yields

$$P_1 - P_2 = Q_t \times \left[ \left( 1 - \frac{Q_c}{Q_t} \right) \times (R_1 + 0.5R_3) - \left( \frac{Q_c}{Q_t} \times R_2 \right) \right], \quad (5)$$

where  $P_1$  and  $P_2$  are the inlet pressures,  $Q_t$  is the total flow rate,  $Q_c/Q_t$  the dilution ratio, and  $R_1$ ,  $R_2$ , and  $R_3$  are the resistances shown in Fig. 1(b). For example, a blood viscosity of 4 cP and a 1:10 dilution ratio needs a 9.1 cmH<sub>2</sub>O difference in height between the reservoirs. If the recalcification buffer reservoir connected to inlet 2 were set to 10 cm H<sub>2</sub>O, the reservoir containing blood would need a head pressure of 19.1 cm H<sub>2</sub>O, or 18 cm of blood using a whole blood specific gravity of 1.06. The blood reservoir in our whole blood assay experiment was therefore initially set at 18 cm above the mixer.

## B. Platelets are neither activated nor accumulated in the mixer

A marker of platelet activation is a shift in the integrin  $\alpha_{IIb}\beta_3$  receptor to its high affinity state.<sup>38</sup> The PAC-1 antibody we used selectively binds to an epitope near the fibrinogen binding site on  $\alpha_{IIb}\beta_3$  in its high affinity state.<sup>39</sup> Alternatively, surface expression of P-selectin (CD62P) is a marker of platelet activation.<sup>39,40</sup>

The mixer was operated in push mode (B) to allow for collection of whole blood emanating from the mixer with no prothrombotic substrate. The flow rate of citrated whole blood was 8.9  $\mu$ l/min, and the flow rate of the recalcification buffer was 0.89  $\mu$ l/min. The mixer was run continuously for 30 min, and PAC-1 binding and anti-CD62P was measured at different time points (Fig. 5 and Supplementary Fig. 3).<sup>41</sup> The percent of PAC-1 positive platelets in the effluent recalcified whole blood was comparable to the unactivated controls and is significantly less than platelets activated by 0.3  $\mu$ M  $\alpha$ -thrombin. The percent of collected CD62P positive platelets was also comparable to the unactivated control. Based on the channel dimensions and flow rates, platelets experience shear stresses of around 10 dyn/cm<sup>2</sup> with an average residence time of 20 s in the mixer. This shear stress and time is less than the 83 dyn/cm<sup>2</sup> known to cause shear induced platelet activation over 180 s.<sup>29</sup>

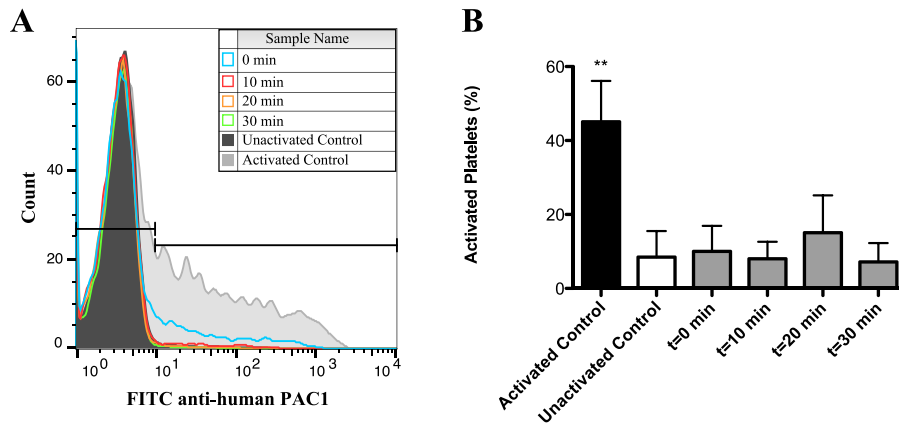


FIG. 5. Measurement of platelet activation in the mixer. (a) Gating of representative flow cytometry samples for platelet activation measurements. Bars represent the two populations of platelets, unactivated on the left, and activated on the right as measured PAC-1 binding. (b) Platelet activation for the activated control ( $0.3 \mu\text{M}$   $\alpha$ -thrombin), unactivated controls (no agonist), and from whole blood collected from the outlet of the flow assay device at various time points. Bars show the mean and the error bars show standard deviation ( $n = 5$ ). Only the activated control (\*) is significantly different ( $p < 0.05$ ) from the samples.

Direct observation of the mixer under operating conditions found one stagnation point, in inlet 1 where the streams split. No platelet buildup or fibrinogen accumulation was observed at the stagnation point over 30 min. The herringbone grooves and corners induced zones of low flow, but no stagnation points were observed. There is a negligible accumulation of labeled fibrinogen based on fluorescence intensity over the 30 min (Supplementary Fig. 4).<sup>41</sup> There was an increase in the mitochondrial membrane dye DiOC6 (Supplementary Fig. 4).<sup>41</sup> However, this increase was likely due to free dye absorbing into the PDMS as brightfield images confirmed no platelet accumulation in the device.

### C. Whole blood flow assay using herringbone mixer for recalcification

Flow assays using batch and continuous recalcification were performed over a collagen-TF surface at a wall shear rate of  $750 \text{ s}^{-1}$  in the flow device. Final calcium and magnesium ion concentrations of  $7.5 \text{ mM}$  and  $3.8 \text{ mM}$  were used to match physiological levels.<sup>11</sup> Using batch recalcification, platelet aggregates were observed to emanate upstream of the collagen-TF strip after 5 min and the channel was almost occluded by 8 min. Supplementary video 1<sup>41</sup> shows that the

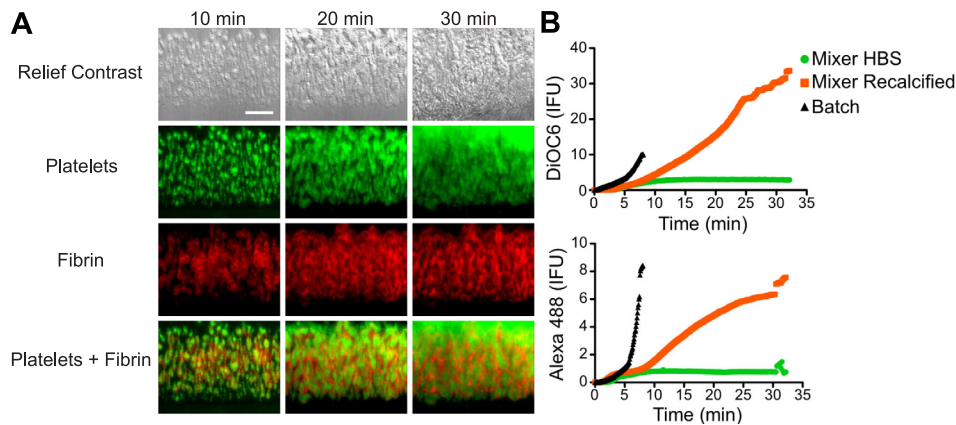


FIG. 6. Batch mixing versus continuous mixing in whole blood flow assay. (a) Images of a flow assay on a fibrillar collagen and TF surface taken at 10, 20, and 30 min and a wall shear rate of  $750 \text{ s}^{-1}$  using relief contrast and epifluorescence. Scale bar =  $100 \mu\text{m}$ . (b) Representative platelet (top) and fibrin (bottom) accumulation for batch recalcification, recalcification through the mixer, and dilution with HBS buffer (no divalent cations) through the mixer.

accumulation of platelets at later times was mostly from deposition of preformed platelet aggregates. This observation is reflected in the rapid accumulation in platelet and fibrin at  $\sim 5.5$  min (Fig. 6). In contrast, continuous recalcification in the mixing device led to gradual accumulation of platelet and fibrin up to 30 min (Fig. 6 and Supplementary video 2).<sup>41</sup> There was no evidence of upstream platelet aggregation using the mixer. When the recalcification buffer was replaced with HBS, platelets still adhered, but did not aggregate and no fibrin formed as expected in the absence of physiological concentrations of divalent cations (Supplementary Figure 1 and Supplementary video 3).<sup>41</sup> The lag time to 5% surface coverage was  $44 \pm 4$  s for batch recalcification, and  $110 \pm 70$  s and  $140 \pm 26$  s for continuous mixing with recalcification buffer and HBS, respectively. This lag time is likely related to the time needed for von Willebrand Factor to adsorb onto collagen.<sup>9</sup> The growth rate up to 5 min was similar for all three methods;  $2.15 \pm 0.79 \times 10^{-3} \text{ s}^{-1}$ ,  $2.14 \pm 0.75 \times 10^{-3} \text{ s}^{-1}$ , and  $1.54 \pm 0.09 \times 10^{-3} \text{ s}^{-1}$  for the batch mixing, continuous mixing with recalcification buffer, and continuous mixing with HBS. However, after 5 min the batch mixing led to rapid growth, the continuous mixing with recalcification buffer led to steady, sustained growth for up to 30 min; and growth ceased with continuous mixing with HBS following an initial layer of platelet adhesion to the surface.

Flow assays that use citrated whole blood are typically run for 3–10 min.<sup>6,9</sup> As evidenced in our batch recalcification experiments, premature platelet activation and aggregation can limit the duration of this mixing approach. Indeed, even if the assay is terminated early prior to occlusion or the rapid thrombus growth phase, batch recalcification might induce artifacts in platelet accumulation. Continuous recalcification through the mixer allows for steady thrombus growth that extends up to at least 30 min. Longer assay times may be feasible, but we limited experiments to 30 min because this is the time when the clot came close to occluding the channel.

#### IV. CONCLUSION

The herringbone mixer described in this report enables the continuous recalcification of citrated whole blood. Platelets are not activated upon perfusion through the mixer, and platelet adhesion and fibrin deposition steadily accumulate on a prothrombotic surface of collagen and TF. Compared to batch recalcification methods, we have tripled the time we can run a coagulation assay. This prolonged duration facilitates the investigation of phenomena such as fibrinolysis and thrombus remodeling that occur over longer time scales. Since the mixer is an independent device, it can be connected to the variety of commercial and custom flow chambers currently used in flow assay studies.

#### ACKNOWLEDGMENTS

This work was supported by NSF CAREER (CBET-1351672) and REU (EEC-115745) grants, the American Heart Association (14GRNT20410094), and the National Institutes of Health (R01HL120728 and R21NS082933).

- <sup>1</sup>A. L. Fogelson and K. B. Neeves, *Annu. Rev. Fluid Mech.* **47**, 377 (2014).
- <sup>2</sup>Z. M. Ruggeri and G. L. Mendolicchio, *Circ. Res.* **100**, 1673 (2007).
- <sup>3</sup>X. Zhang, K. Halvorsen, C. Z. Zhang, W. P. Wong, and T. A. Springer, *Science* **324**, 1330 (2009).
- <sup>4</sup>A. A. Onasoga Jarvis, T. J. Puls, S. K. O'Brien, L. Kuang, H. J. Liang, and K. B. Neeves, *J. Thromb. Haemostasis* **12**, 373 (2014).
- <sup>5</sup>D. Repke, C. H. Gemmell, A. Guha, V. T. Turitto, J. G. J. Broze, and Y. Nemerson, *Proc. Natl. Acad. Sci.* **87**, 7623 (1990).
- <sup>6</sup>K. B. Neeves and S. L. Diamond, *Lab Chip* **8**, 701 (2008).
- <sup>7</sup>R. R. Hansen, A. R. Wufsus, S. T. Barton, A. A. Onasoga, R. M. Johnson-Paben, and K. B. Neeves, *Ann. Biomed. Eng.* **41**, 250 (2013).
- <sup>8</sup>R. R. Hansen, A. A. Tipnis, T. C. White-Adams, J. A. Di Paola, and K. B. Neeves, *Langmuir* **27**, 13648 (2011).
- <sup>9</sup>K. B. Neeves, A. A. Onasoga, R. R. Hansen, J. J. Lilly, D. Venckunaite, M. B. Sumner, A. T. Irish, G. Brodsky, M. J. Manco-Johnson, and J. A. Di Paola, *PLoS ONE* **8**, e54680 (2013).
- <sup>10</sup>S. M. de Witt, F. Swieringa, R. Cavill, M. M. E. Lamers, R. Van Kruchten, T. Mastenbroek, C. Baaten, S. Coort, N. Pugh, A. Schulz, I. Scharrer, K. Jurk, B. Zieger, K. J. Clemetson, R. W. Farndale, J. W. M. Heemskerk, and J. M. E. M. Cosemans, *Nat. Commun.* **5**, 1 (2014).
- <sup>11</sup>R. Van Kruchten, J. M. E. M. Cosemans, and J. W. M. Heemskerk, *Platelets* **23**, 229 (2012).

- <sup>12</sup>E. Westein, S. De Witt, M. Lamers, J. M. E. M. Cosemans, and J. W. M. Heemskerk, *Platelets* **23**, 501 (2012).
- <sup>13</sup>T. V. Colace, G. W. Tormoen, O. J. T. McCarty, and S. L. Diamond, *Ann. Rev. Biomed. Eng.* **15**, 283 (2013).
- <sup>14</sup>S. M. Baker, K. G. Phillips, and O. J. T. McCarty, *Cel. Mol. Bioeng.* **5**, 488 (2012).
- <sup>15</sup>D. P. Sarvepalli, D. W. Schmidtke, and M. U. Nollert, *Ann. Biomed. Eng.* **37**, 1331 (2009).
- <sup>16</sup>J. Yu, D. Tao, E. X. Ng, C. L. Drum, A. Q. Liu, and C.-H. Chen, *Biomicrofluidics* **8**, 052108 (2014).
- <sup>17</sup>S. Meyer dos Santos, A. Zorn, Z. Guttenberg, B. Picard-Willems, C. Kläffling, K. Nelson, U. Klinkhardt, and S. Harder, *Biomicrofluidics* **7**, 056502 (2013).
- <sup>18</sup>H. Song, H.-W. Li, M. S. Munson, A. Thuong, G. Van Ha, and R. F. Ismagilov, *Anal. Chem.* **78**, 4839 (2006).
- <sup>19</sup>C. H. Lin, C. Y. Liu, C. H. Shih, and C. H. Lu, *Biomicrofluidics* **8**, 052105 (2014).
- <sup>20</sup>A. A. Onasoga, K. Leiderman, A. L. Fogelson, M. Wang, M. J. Manco-Johnson, J. A. Di Paola, and K. B. Neeves, *PLoS ONE* **8**, e78732 (2013).
- <sup>21</sup>K. B. Neeves, O. J. T. McCarty, A. J. Reininger, M. Sugimoto, and M. R. King, *Biorheology Subcommittee, J. Thromb. Haemostasis* **12**, 418 (2014).
- <sup>22</sup>K. G. Mann, M. F. Whelihan, S. Butenas, and T. Orfeo, *J. Thromb. Haemostasis* **5**, 2055 (2007).
- <sup>23</sup>H. A. Stone, A. D. Stroock, and A. Ajdari, *Annu. Rev. Fluid Mech.* **36**, 381 (2004).
- <sup>24</sup>J. Marschewski, S. Jung, P. Ruch, N. Prasad, and S. Mazzotti, *Lab Chip* **15**, 1923 (2015).
- <sup>25</sup>J. M. Ottino and S. Wiggins, *Philos. Trans. R. Soc. London, Ser. A* **362**, 923 (2004).
- <sup>26</sup>D. N. Bell, S. Spain, and H. L. Goldsmith, *Biophys. J.* **56**, 817 (1989).
- <sup>27</sup>A. D. Stroock, S. K. W. Dertinger, A. Ajdari, I. Mezić, H. A. Stone, and G. M. Whitesides, *Science* **295**, 647 (2002).
- <sup>28</sup>R. W. Muthard and S. L. Diamond, *Biorheology* **51**, 227 (2014).
- <sup>29</sup>H. Shankaran, P. Alexandridis, and S. Neelamegham, *Blood* **101**, 2637 (2003).
- <sup>30</sup>K. W. Oh, K. Lee, B. Ahn, and E. P. Furlani, *Lab Chip* **12**, 515 (2012).
- <sup>31</sup>M. R. Barnard, L. A. Krueger, A. L. Freilinger III, and M. I. Furman, *Platelets* **20**, 279 (2002).
- <sup>32</sup>C. A. Schneider, W. S. Rasband, and K. W. Eliceiri, *Nat. Meth.* **9**, 671 (2012).
- <sup>33</sup>K. B. Neeves, S. F. Maloney, K. P. Fong, A. A. Schmaier, M. L. Kahn, L. F. Brass, and S. L. Diamond, *J. Thromb. Haemostasis* **6**, 2193 (2008).
- <sup>34</sup>D. D. Nalayanda, M. Kalukanimuttam, and D. W. Schmidtke, *Biomed. Microdevices* **9**, 207 (2007).
- <sup>35</sup>K. Aran, L. A. Sasso, N. Kamdar, and J. D. Zahn, *Lab Chip* **10**, 548 (2010).
- <sup>36</sup>R. Fåhræus and T. Lindqvist, *Am. J. Physiol.* **96**, 562 (1931).
- <sup>37</sup>A. R. Pries, D. Neuhaus, and P. Gahtgens, *Am. J. Physiol. - Heart Circ. Physiol.* **263**, H1770 (1992).
- <sup>38</sup>S. J. Shattil, J. A. Hoxie, M. Cunningham, and L. F. Brass, *J. Biol. Chem.* **260**, 11107 (1985).
- <sup>39</sup>A. D. Michelson, *Am. J. Cardiol.* **103**, 20A (2009).
- <sup>40</sup>J. L. Ritchie, H. D. Alexander, and I. M. Rea, *Clin. Lab. Haematol.* **22**, 359 (2000).
- <sup>41</sup>See supplementary material at <http://dx.doi.org/10.1063/1.4935863> for supplementary figures and media.